dendritic arms seen in the traditional DLA were allowed to wiggle, the diffuse structure would collapse and become more compact.

Thus, it is the wiggling of the partially frozen chains, which in turn allows these chains to form self-loops and bind with other partially frozen chains, that makes the resulting cluster fundamentally different from that seen in small-particle DLA. This difference is reflected in the different scaling behavior.

Conclusions

We have performed a Monte Carlo simulation in two dimensions of the diffusion-limited aggregation of monodisperse associating polymer chains. The chains can aggregate only through their ends. Except for the seed chain, the dynamics of the chains have been simulated using the Verdier–Stockmayer algorithm. Each member chain is free to move until both ends of the chain are anchored to the growing aggregate. The dependence of the radius of gyration of the aggregate on the chain length and the number of chains has been investigated.

First, we demonstrate that our diffusion-limited network formation is distinctly different from the small-particle diffusion-limited aggregation. By assuming that the monomer concentration of our aggregate is comparable to the monomer concentration at the overlap threshold for a solution of two-dimensional self-avoiding chains, we have been able to correlate the radius of gyration of the cluster with the chain length and the number of chains in the aggregate. The presence of self-loops causes the cluster to contract in the size and results in a small deviation from the predicted exponent relating the radius of gyration and the number of chains.

Acknowledgment. This work was supported by NSF Grant DMR8420962 and the Center for UMass-Industry Research in Polymers. Anna C. Balazs and Charles Anderson greatly acknowledge contributions from Frank E. Karasz, under Grant AFOSR 85-01000.

References and Notes

(1) MacKnight, W. J.; Earnest, T. R. *Macromol. Rev.* **1981**, *16*, 41.
(2) Eisenberg, A. *J. Polym. Sci., Polymer Symp.* **1974**, *45*, 99.
(3) Eisenberg, A. *Macromolecules* **1970**, *3*, 147.
(4) Duvdevani, I.; Agarwal, P. K.; Lundberg, R. D. *Polym. Eng. Sci.* **1982**, *22*, 499.
(5) Weiss, R. A.; Lundberg, R. D.; Werner, A. *J. Polym. Sci., Polym. Chem. Ed.* **1980**, *18*, 3427.
(6) Rahrig, D.; MacKnight, W. J.; Lenz, R. W. *Macromolecules* **1979**, *12*, 195.
(7) Mohajer, Y.; Bagrodia, S.; Wilkes, G. L.; Storey, R. F.; Kennedy, J. P. *J. Polym. Sci., Polym. Symp.* **1984**, *29*, 1943.
(8) Broze, C.; Jerome, R.; Teyssie, P. *J. Polym. Sci., Polym. Lett. Ed.* **1981**, *19*, 415.
(9) Hegedus, R. D. Ph.D. Dissertation, University of Massachusetts, Cambridge, 1985.
(10) Kreuder, W.; Ringsdorf, H.; Tschirner, P. *Makromol. Chem., Rapid Commun.* **1985**, *6*, 367.
(11) Stauffer, D.; Coniglio, A.; Adam, M. *Adv. Polym. Sci.* **1982**, *44*, 103.
(12) Eicke, H.-F. In *Micelles*; Springer-Verlag; Berlin, 1980; p 85.
(13) Witten, T. A.; Cohen, M. H. *Macromolecules* **1985**, *18*, 1915.
(14) Family, F.; Landau D. P. *Kinetics of Aggregations and Gelation*; North-Holland: New York, 1984.
(15) Verdier, P. H.; Stockmayer, W. H. *J. Chem. Phys.* **1962**, *36*, 227.
(16) Domb, C. *Adv. Chem. Phys.* **1962**, *15*, 229.
(17) Hilhorst, H. J.; Deutch, J. M. *J. Chem. Phys.* **1975**, *63*, 5153.
(18) Baumgartner, A. *Ann. Rev. Phys. Chem.* **1984**, *35*, 419.
(19) Flory, P. J. *Principles of Polymer Chemistry*; Cornell University Press: Ithaca, NY, 1953; Chapter 13.
(20) deGennes, P. G. *Scaling* Concepts *in Polymer Physics*; Cornell university Press: Ithaca, NY, 1979.

Physical Gelation of a Multiblock Copolymer

Xiongwei He, Jean Herz, and Jean-Michel Guenet*

Institut Charles Sadron (CRM-EAHP), CNRS-Université Louis Pasteur, 67083 Strasbourg, Cedex, France. *Received December 3, 1986*

ABSTRACT: The thermoreversible gelation of a multiblock copolymer made up of poly(dimethylsiloxane) blocks ("soft" segments) and poly[(dimethylsilylene)phenylene(dimethylsilylene)-1,2-ethanediyl] blocks ("hard" segments) is studied. The thermal behavior as a function of polymer concentration is investigated which allows the phase diagram to be established. This phase diagram shows the occurrence of a monotectic transition which implies that the gel formation proceeds from a liquid–liquid phase separation frozen in at its early stage by crystallization. The mechanical properties through the determination of the compression modulus E are examined. It is found that the knowledge of the phase diagram enables one to account for the variation of E with temperature. This result leads to the conclusion that gel partial melting takes place at the monotectic transition rather than the abrupt disappearance of one type of crystal. Finally, swelling experiments are interpreted by means of a model involving microfibrils instead of the usual fringed micelle model.

Introduction

Physical gels constitute a particular class of materials. Numerous investigations carried out on gels from homopolymers are now available.[1-6] Yet, as far as copolymers are concerned, only a few studies have been reported. Berghmans et al.[7] have studied statistical copolymers (poly[(ethylene terephthalate)-*co*-isophthalate]) as have Takahashi and Mandelkern et al.[8] [poly(ethylene–butadiene) and poly[ethylene–(vinyl acetate)]]. To our knowledge, no extensive study dealing with multiblock copolymers, where crystalline and amorphous sequences alternate, have been achieved hitherto. This type of copolymer possesses some interesting particularities which can provide information on gelation as a whole. For instance, beyond a certain number of sequences the copolymer behaves in a homopolymer-like fashion. Thereby, light may be thrown on gelation of atactic polymers containing some stereoregular sequences. In addition, the synthesis procedure allows the composition and the average length of both or either sequence to be varied.

The purpose of this paper is to report on the thermal analysis and the phase diagram, the mechanical properties, and the swelling behavior of an organosilicic block copolymer. This study gives a new approach to the gel melting mechanism and shows that the mechanical properties as well as the swelling behavior can be accounted

0024-9297/87/2220-2003$01.50/0

for by simple phenomenological theories whose parameters are given by the experimental phase diagram.

Experimental Section

(1) Synthesis. The material used for the present study is a multiblock copolymer in which are associated flexible poly(dimethylsiloxane) blocks (PDMS) and crystallizable "hard" blocks of poly[(dimethylsilylene)phenylene(dimethylsilylene)-1,2-ethanediyl]. The crystalline block will be designated as COSP throughout the paper (crystalline organosilicic polymer).

The synthesis of these block copolymers has been first described by Prud'homme.[9,10] The method used is schematically represented below:

$$N_A[\underset{A}{HSi(CH_3)_2C_6H_4Si(CH_3)_2H}] + N_B[\underset{B}{CH_2{=}CHSi(CH_3)_2C_6H_4Si(CH_3)_2CH{=}CH_2}] \xrightarrow[\text{toluene}]{H_2PtCl_6}$$
$$\underset{\text{COSP}}{CH_2{=}CH{-}[Si(CH_3)_2C_6H_4Si(CH_3)_2CH_2CH_2]_n{-}Si(CH_3)_2C_6H_4Si(CH_3)_2{-}CH{=}CH_2} + N[HSi(CH_3)_2{-}(OSi(CH_3)_2)_x{-}Si(CH_3)_2H] \rightarrow$$
$$-[(OSi(CH_3)_2)_x(CH_2CH_2Si(CH_3)_2C_6H_4Si(CH_3)_2)_y]_n-$$

It is entirely based on the hydrosilylation reaction. The synthesis has to be carried out under well-defined experimental conditions or else side reactions take place[11-13] which in some cases can yield very high molecular weights as well as branched species. A deeper investigation dealing with this problem enabled one to define the optimal experimental conditions that avoid the aforementioned problems.[14]

Accordingly, the following procedure was used: in a first step, a crystallizable precursor polymer (POSC) with silylvinylic end group was prepared by using an excess of compound B. The stoichiometric ratio $r = N_A/N_B$ is fixed in accordance with the desired molecular weight. The reaction is carried out in dried toluene (distilled on sodium wires) at a concentration corresponding to 330 g/L. After 1 h of reaction at 90 °C, an almost quantitative yield is obtained and the molecular weight of the polymer formed is close to the theoretically expected value.[15] This telechelic COSP is kept in toluene at 90 °C while a solution of α,ω-functional PDMS of known molecular weight in toluene at the same concentration is added to it followed by a second addition of catalyst. The amount of PDMS added is chosen in such a way that the total stoichiometric ratio r_t reads

$$r_t = (N_A + N)/N_B = 1$$

After an additional 2 h of reaction, the product is recovered by precipitation into methanol, filtered, washed, and carefully dried under vacuum at 60 °C.

The condensation reaction gives a block copolymer containing 10–12 blocks which shows an elastic behavior when the fraction of PDMS exceeds approximately 60% (w/w). In this study only one composition has been investigated, namely, 80% PDMS–20% COSP.

(2) Characterization. Light-scattering and gel permeation chromatography (GPC) were used to determine the different molecular weight averages.

Light-scattering measurements were carried out on a FICA 50 at 60 °C in toluene with a vertically polarized laser light of 546-nm wavelength. As the weight average molecular weight M_w determined in one solvent is virtually the actual one with a multiblock copolymer, no other solvent was used. Refractive index increments dn/dC were measured by means of a Brice-Phoenix refractometer under the same conditions. The following results were obtained: $M_w = 1.3 \times 10^5$ and $dn/dC = -0.06$. This latter value does agree with a composition of the copolymer corresponding to 20% COSP and 80% PDMS.

GPC characterization was achieved at room temperature in toluene with a WISP 710B equipped with a refractometer from SHIMAZU. Columns were calibrated with polystyrene standards of very low polydispersity. The results were $M_w = 1.1 \times 10^5$, $M_n = 6.2 \times 10^4$, and $M_w/M_n = 1.8$.

As can be seen, the agreement is quite good between the weight-average molecular weights determined by either technique. The polydispersity of nearly 2 corresponds to what is normally expected for polycondensation.

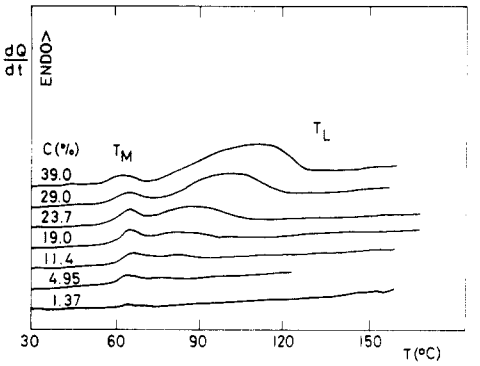

Figure 1. DSC thermograms (20 °C/min) of mixtures COSP + *trans*-decalin prepared by heating at 180 °C to ensure homogeneity then quenched at −18 °C for 24 h and annealed at 30 °C for 7 days. Concentrations are given in weight percent.

From these results, it is deduced that the copolymer is constituted of approximately 12 blocks (taking the weight-average molecular weight). This justifies a posteriori the molecular weight characterization in only one solvent.

(3) Techniques and Sample Preparation. High-purity grade *trans*-decalin was used as the solvent throughout this study.

(a) Thermal Analysis. Test tubes containing homogeneous solutions were quenched into iced water to produce gels. Approximately 10 mg of this freshly prepared gel was then placed into an aluminum "volatile sample" pan which was hermetically sealed. The sample was heated up to 150 °C to remelt the gel, then quenched again at −18 °C, and kept at that temperature for 24 h. Finally, the samples were annealed at 30 °C for a week. This last step turned out to appreciably improve the quality and resolution of the DSC thermograms without significantly altering T_M and T_L. The pans were weighed after each experiment to detect any loss of solvent.

The same type of investigation was made with the crystalline block alone in the presence of *trans*-decalin. The samples were prepared under exactly the same conditions.

DSC II and DSC 4 calorimeters from Perkin-Elmer were used. All the data were processed by means of the TADS system (thermal analysis data station). Experiments were performed at different heating rates. However, the standard 20 °C/min heating rate was employed to establish the phase diagrams. Calibrations were achieved with an indium standard.

To make the solvent crystallize in the gel samples, low cooling rates were used (typically −2.5 to −1 °C/min).

(b) Mechanical Properties. A mold with parallel surfaces was used to produce slabs of gel of 1-cm thickness. These slabs were thermally treated exactly as above. Afterwards, cylinders of 1.5-cm diameter were cut off to perform the mechanical measurements.

The compression moduli determination was carried out with a device described elsewhere.[16] The gels were kept immersed in water thermostatically controlled by an outer water circulation. Decalin and water are totally incompatible which results in the absence of any alteration of the piece of gel. This procedure avoids the use of an excess of preparation solvent which would inevitably affect the degree of swelling of the gel and correspondingly its mechanical response with time.

Results and Discussion

I. Thermal Behavior and Phase Diagram. The gel thermal behavior is inevitably related to the properties of the crystalline block. It is therefore felt that a study of the crystalline block in the same solvent as that used to form the copolymer gel is needed.

(1) Crystalline Block. Typical DSC traces of COSP + *trans*-decalin blends prepared as described above are drawn in Figure 1. These thermograms reveal two endotherms: a low-melting endotherm whose position T_M does not move with concentration and a high-melting endotherm the maximum of which shifts toward higher temperature for increasing concentration. While the low-

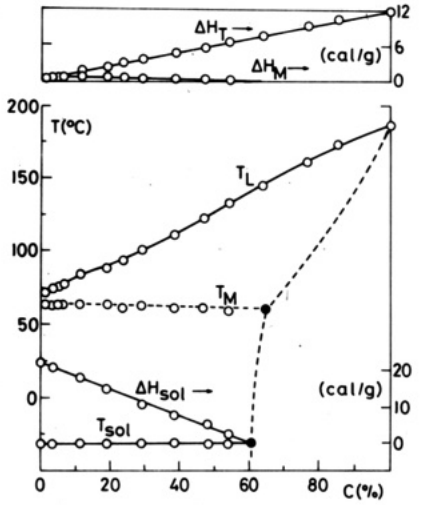

Figure 2. Phase diagram established from the data of Figure 1 and those obtained on the solvent crystallization. Enthalpies of both first transition endotherms are also given. Concentrations in weight percent.

melting endotherm fades out at higher concentrations and becomes actually zero for $C \simeq 60\%$, the high-melting endotherm area continuously increases.

The temperature–concentration phase diagrams of Figure 2 is obtained by plotting the temperature T_M (maximum of the low-melting endotherm), T_L (end of the high-melting endotherm), and T_{sol} (solvent melting temperature). On this diagram are also given the different enthalpies as a function of concentration (ΔH_M = low-melting endotherm, ΔH_T = total melting areas, and ΔH_{sol} = solvent melting).

From this phase diagram, two conclusions can be drawn.

(i) The invariance of T_M can only be accounted for by three cases: formation of a eutectic, of a peritectic, or of a monotectic system. The melting points of the polymer and the solvent are too different so that no eutectic can be formed at that temperature. The peritectic system should also form on slow cooling which is not the case. Accordingly, a monotectic system is formed which is characterized by a transition of the type solid + liquid 1 ↔ solid + liquid 2 (with concentration of liquid 1 lower than that of liquid 2). Such a transition arises from the mechanism of crystal formation which can be described as a liquid–liquid phase separation occurring prior to crystallization. Phase separation of this kind produces a polymer-rich phase of always the same concentration for a given temperature of quench regardless of the initial concentration, hence the invariance of T_M.[17] This monotectic transition is only seen when a rapid quench is brought about but disappears for slowly cooled systems. This means that the miscibility gap lies at lower temperature than T_M does. It is known from energetic considerations[18] that once the solution has reached, unaltered, the miscibility gap, liquid–liquid phase separation is compulsory and takes place before crystallization. Obviously, there can exist a discrepancy between the temperature of crystallization (the latter taking place within the miscibility gap) and the melting temperature (which is determined by crystal thickness). Accordingly, the monotectic line can be situated well above the miscibility gap which is the situation encountered here.

To back up the above explanation, the morphology of crystals grown from dilute solutions has been determined. As a matter of fact, usual crystallization produces flat and thin crystals (typically 100-Å thickness) whereas it has been recently demonstrated[19] that crystallization occurring after liquid–liquid phase separation produces globelike crystals (diameter of about 0.1–1 μm).

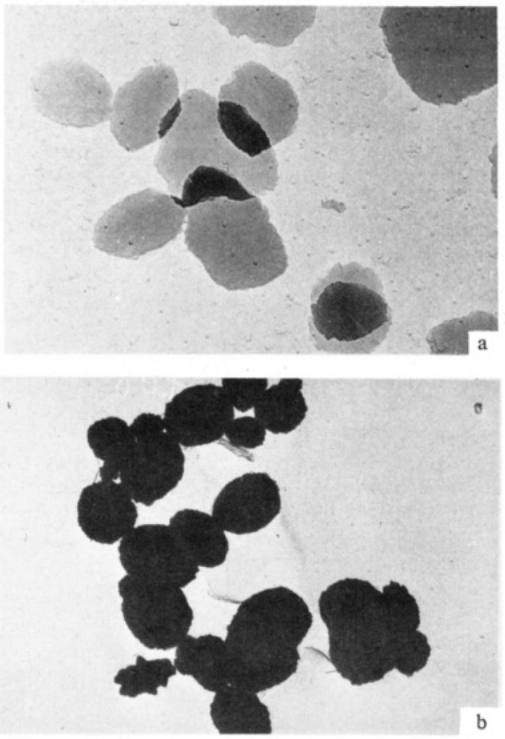

Figure 3. Electron micrographs of the species obtained by crystallization of 1% COSP solutions in *trans*-decalin: (a) quenched at 60 °C; (b) quenched at −18 °C.

This is illustrated in Figure 3 which shows crystals grown from 1% solutions annealed at 60 °C (Figure 3a) and −18 °C (Figure 3b), respectively.

(ii) From the concentration C_0 determined at $\Delta H_{sol} = 0$, a parameter α can be defined[20] which stands for the number of solvent molecules bound per monomeric unit. (There is always a specific interaction between the polymer and the solvent leading to what is sometimes referred to as the "depletion layer". In this depletion layer, the solvent possesses liquid behavior even well below its crystallization temperature.) This parameter simply reads

$$\alpha = [(1 - C_0)/C_0](m_P/m_s) \quad (1)$$

where m_P and m_s are the molecular weights of the monomer and the solvent respectively.

The value $\alpha \simeq 1$ found is rather high, a result which might be consistent with a polymer–solvent compound. While the phase diagram would also suggest the existence of such a compound (in particular ΔH_M and ΔH_{sol} become zero at approximately the same concentration), preliminary X-rays investigations[21] do not show a significant difference between a 50%- and a bulk-crystallized COSP samples. It will be provisionally admitted that the system rather forms a solid solution, the structure of which remains to be elucidated.

(2) Copolymer. DSC thermograms are drawn in Figure 4 for different copolymer concentrations. As in the case COSP + *trans*-decalin, for $C > C_M$, the low-melting endotherm position is invariant with concentration whereas the high-melting endotherm maximum shifts toward higher temperature. Interestingly, for $C < C_M$, only the low-melting endotherm is observed. As above, a phase diagram can be established (Figure 5) (here the monotectic temperature is taken as the onset of the low-melting endotherm).

In this system, the monotectic point is well evidenced. In particular, the increase of the low-melting area up to

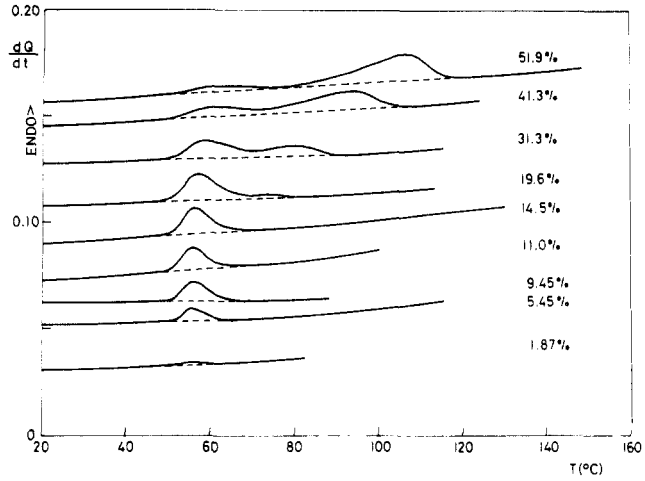

Figure 4. DSC thermograms obtained at 20 °C/min for the copolymer gels prepared by quenching homogeneous solutions at −18 °C for 24 h and then annealing for 7 days at 30 °C. Concentrations are given in weight by weight.

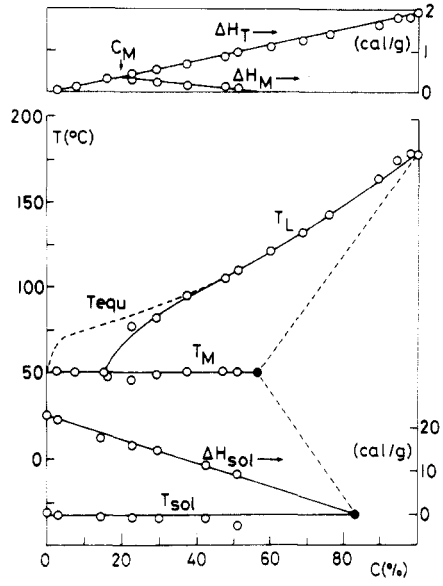

Figure 5. Phase diagram established from the data of Figure 4 and the crystallization of the solvent. Enthalpies of the first-order transition endotherms are also given. As previously, concentrations are in weight percent. T_{equ} is the melting temperature for slowly crystallized systems.

C_M ($C_M \simeq 0.18$) and its decrease down to C_α ($C_\alpha \simeq 0.55$) is clearly and unambiguously pointed out. Here, the phase diagram shows the formation at higher concentration of a solid solution. Such a result is not surprising since the solvent can be trapped within the amorphous part of the polymer-rich phase which was not possible with the crystalline COSP. As to a possible polymer–solvent compound in the crystalline domain of the polymer-rich phase, its existence would still be more difficult to evidence since the crystalline component represents only 20% of the copolymer. Paradoxically, while decalin is a good solvent of PDMS, there is less solvent bound at the solvent crystallization temperature than there was previously.

The observation of a monotectic line implies that the system copolymer + *trans*-decalin possesses a miscibility gap. As decalin is a good solvent for PDMS, this entails that the solution properties of the copolymer are mainly determined by the crystalline block despite its low proportion.

At this stage of the discussion, it is of importance to dwell upon the fact that T_M does not necessarily represent the melting of one type of crystals and T_L that of another type. Due to gel formation within a miscibility gap, thermodynamics requires that at a given temperature part of the material melt. That this part be a certain type of crystals cannot be said. Actually, the results obtained from compression measurements are rather consistent with a partial melting of the same type of crystals.

To summarize, when the solution is quenched rapidly at low temperature (i.e., well-below room temperature), the gelation mechanism proceeds from a liquid–liquid phase separation frozen in at its early stage by crystallization. Such a mechanism has already been proposed for homopolymers.[2]

Unlike isotactic polystyrene, for which it is strongly suspected that the gels are not of crystalline nature,[20] gels studied here owe their physical cross-links to crystallization as hinted by preliminary X-rays experiments[21] (the strongest reflections are the same in bulk-crystallized COSP and in the dried gel). Further, the total melting enthalpy ΔH_T extrapolates for $C = 1$ to the value expected for the COSP block being totally crystallized (theoretical value $\Delta H = 2.36$ cal/g; actual result $\Delta H \simeq 2$ cal/g).

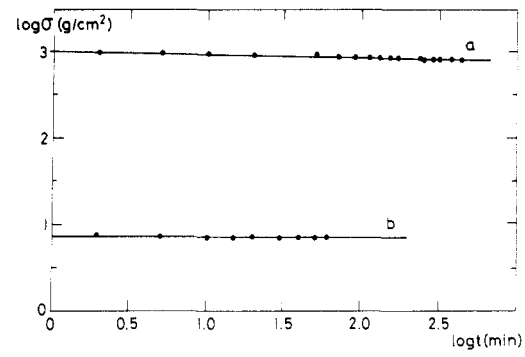

Figure 6. Stress relaxation log σ vs. log t for $\Delta\lambda/\lambda = 0.9$: (a) $C = 0.45$; (b) $C = 0.16$.

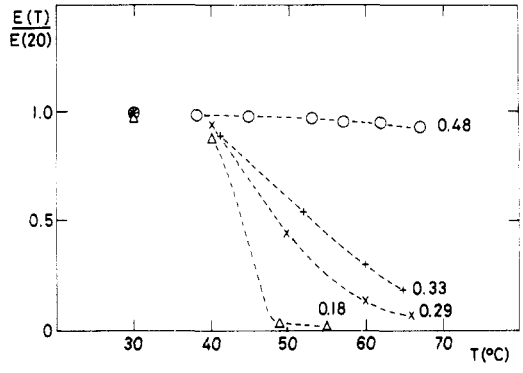

Figure 7. Reduced modulus $E(T)/E(20)$ as a function of temperature T. Concentrations are given in weight percent.

II. Mechanical Behavior. Compression Modulus. In Figure 6 are represented the stress relaxations at constant deformation λ ($\lambda = \Delta l/l = 0.9$). The relaxation rate $m = \mathrm{d}\log\sigma/\mathrm{d}\log t$ (σ = stress and t = time) is on the order of $m \simeq 0.023$–0.035. These values are reminiscent of what is usually found for swollen rubbers[22] but contrasts with recent results gained on isotactic polystyrene[23] ($m \simeq 0.1$–0.15). The fact that iPS gels are said to be noncrystalline whereas those herein are crystalline may account for this rather large discrepancy.

(1) Modulus vs. Temperature. Within the limit of small deformations, the compression modulus E reads

$$E = \sigma/(\lambda - 1/\lambda^2) \qquad (2)$$

where λ is the strain and σ the reduced stress.

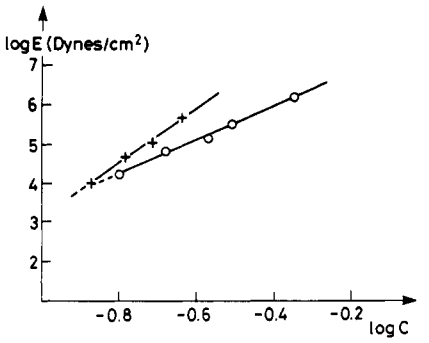

Figure 8. Modulus E vs. concentration C on a logarithmic scale. Open circles stand for the gel as prepared and crosses for the gel swollen at equilibrium in an excess of *trans*-decalin.

Data are given in Figure 7 where $E(T)/E(20)$ is plotted as a function of temperature T ($E(T)$ = modulus at T and $E(20)$ = modulus at 20 °C). As can be seen in Figure 7, there is virtually no variation of E with temperature up to 40 °C. From 40 °C onward, the variation depends on concentration. At low concentrations ($C \simeq C_M$), the modulus drops down quite suddenly which corresponds to the crossing of the monotectic line. For concentrations $C > C_M$, the rate of decay is inversely proportional to concentration. In the appendix is developed a phenomenological theory which is based on the concept of gel partial melting. As can be seen in that section, the modulus–temperature behavior can be reproduced by using the parameters obtained from the phase diagram (C_M, C_α, ...). Although simple and unsophisticated, this theory supports the concept of gel partial melting occurring at T_M rather than the melting of one type of crystals the other one remaining unaltered. Obviously, it cannot be anticipated as to what happens at the molecular level.

(2) Modulus vs. Concentration. Figure 8 depicts the variation of the modulus as a function of polymer concentration at T = 30 °C. From this plot, the following behavior is determined:

$$E \sim C^{4.5\pm0.1} \tag{3}$$

The exponent found is rather high and contrasts with the value expected for systems in good solvents[24] ($\simeq$2.25) that possess a structure close to that of covalent networks. Evidently, the structure and morphology of covalent and physical gels are poles apart. Consequently, it is unrealistic to interpret the results shown here within the frame of theories developed for unlike systems.

After swelling of the gel in an excess of solvent, the difference is still more dramatic since it is found to be

$$E \sim C^{6\pm0.3} \tag{4}$$

III. Swelling Properties. The swelling properties constitute an important chapter of covalent gels[25] which is well documented both from the theoretical and the experimental aspects.

Due to the multiblock characteristic of the copolymer, it is expected that its gels should swell once immersed in an excess of solvent and reach an equilibrium swelling ratio. As outlined above, such is the case.

For the sake of simplicity, the swelling ratio G is taken as

$$G = P/P_0 \tag{5}$$

where P_0 is the sample's weight after preparation but just before immersion in an excess of *trans*-decalin, P is the sample's weight after a certain time. The swelling equilibrium ratio G^∞ is then expressed as

$$G^\infty = (P/P_0)_{t\to\infty} \tag{6}$$

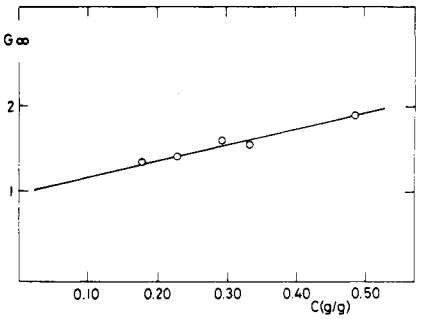

Figure 9. Equilibrium swelling ratio G^∞ as a function of the preparation concentration.

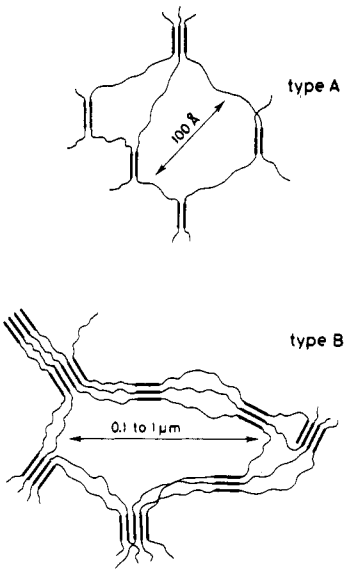

Figure 10. Two schematic types of fringed micelle models: type A is characterized by a short mesh and is thus reminiscent of the structure encountered in covalently cross-linked gels. In this model, two crystalline knots are linked by one and only one disordered chain portion when the connection is direct. Type B is characterized by a larger mesh due to the fact that two consecutive crystalline knots are linked by several disordered chain portions. This results in the formation of small fibers and the existence of totally ineffective physical links.

A first series of experiments has been performed as a function of the preparation concentration C_{prep}. In Figure 9 are plotted values of G^∞ as a function of concentration. For a covalent gel, the "C^* theorem"[24] states that the system should swell up to the (overlap concentration) C^* of the chains joining the knots. C^* reads

$$C^* \simeq M/[(4/3)\Pi R^3 N_A] \tag{6a}$$

where R is the radius of gyration of a chain attached at its both ends to the network, M its molecular weight, and N_A Avogadro's number.

G^∞ should then read

$$G^\infty = C_{prep}/C^* \tag{7}$$

This relation ignores the network defects such as entanglements. It turns out to pertain, however, in a large range of concentration.[26] Should the gels possess a fringed micellar structure of type A (see Figure 10), one would expect it to behave as a covalent gel. The slope of relation 7 which is unity is not found here by taking $C^* = 0.04$[27] for the PDMS block. A slope of about 0.16 is found instead.

The departure from theoretical predictions is too large to be only attributed to defects. This emphasizes again that the gel morphology is too unlike that of covalent gels for theories developed for the latter to be used.

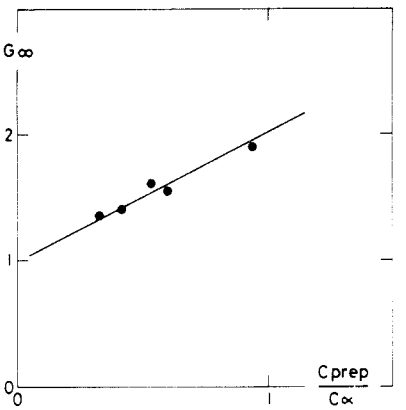

Figure 11. Equilibrium swelling ratio G^{∞} replotted as a function of C_{prep}/C_{α}.

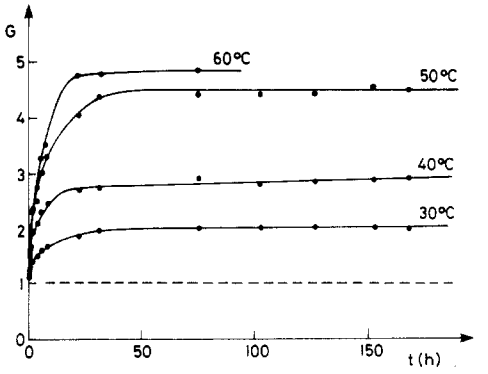

Figure 12. Swelling G ratio as a function of time t for different temperatures $C = 0.48$.

It is known[2,6] that the gel formation mechanism involving a liquid–liquid phase separation produces structures that may be termed as macroscopic (mesh size $\simeq$ 0.1–1 μm) rather than microscopic (as in covalent gels where the mesh size is $\simeq$100 Å). The second model of Figure 10, which can be designated as fringed micellar of type B, is then more appropriate.

On the basis of this model, it can be postulated that only the polymer-rich phase is bound to swell. As the polymer-rich phase has always the same concentration for a given temperature of quench, it should always swell at the same concentration. These assumptions entail that the swelling ratio G^{∞} should be directly proportional to the amount X_{α} of polymer-rich phase. From straightforward arguments detailed in Appendix B, it can be shown that G^{∞} reads

$$G^{\infty} = 1 + (C_{\alpha}/C_{\gamma} - 1)X_{\alpha} \quad (8)$$

where C_{γ} is the concentration reached by the polymer-rich phase after swelling. X_{α} can be approximated to

$$X_{\alpha} \simeq C_{prep}/C_{\alpha} \quad (9)$$

In Figure 11, the results are replotted as a function of C_{prep}/C_{α}. From the slope it is found $C_{\gamma} \simeq 0.27$. Such a value seems relevant and indicates that eq 8 can qualitatively describe the swelling behavior as a function of preparation concentration. Obviously, a deeper knowledge of the gel morphology as a function of concentration is needed to correctly account for the gel swelling behavior as well as its mechanical properties.

A few investigations of the swelling properties as a function of temperature have also been performed. The variation of G as a function of time for different temperatures is given in Figure 12. As can be seen, there is a gap between 40 and 50 °C. A plot of G^{∞} as a function of temperature (Figure 13) points out the existence of a jump which is evidently associated with the monotectic transi-

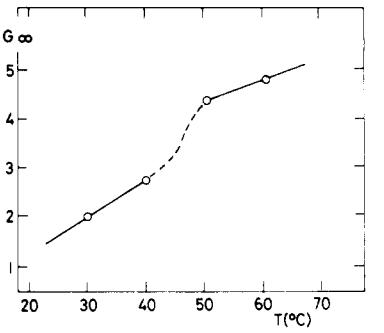

Figure 13. Equilibrium swelling ratio G^{∞} as a function of temperature; $C = 0.48$.

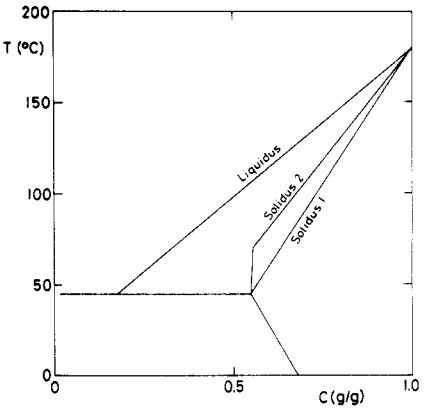

Figure 14. Schematic representation of the phase diagram of Figure 4. All the curves have been approximated to straight lines.

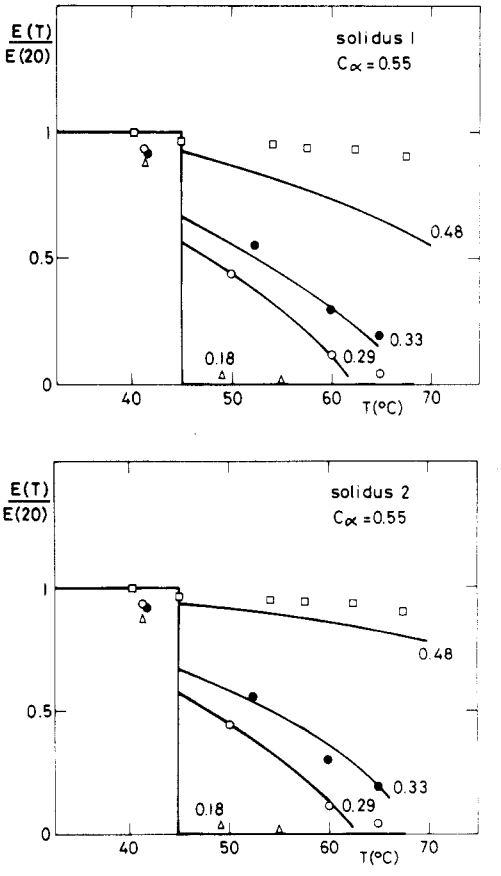

Figure 15. Comparison between the values measured of the compression modulus (in its reduced form as in Figure 7) and those theoretically calculated (bold lines) using the phase diagram of Figure 14 and eq 5A and 6A.

tion. As already stressed above, this "jump" is a further illustration of the concept of partial melting.

Conclusion

The investigation reported here enables one to cast some light on both gel formation mechanism and gel melting process. In addition, gel morphology is outlined on the basis of swelling experiments.

From now on, further studies should deal with the effect of the copolymer composition and the role played by the solvent. Such studies are in progress and will be reported in due course.

Acknowledgment. We are indebted to S. Graff for the electron micrographs.

Appendix A

We choose to express the compression modulus E as follows:

$$E \propto f(C)g(T)h(T) \tag{1A}$$

$f(C)$ depends on the polymer concentration and contains mainly the polymer–solvent interaction effects. $g(T)$ describes the effect of temperature on the flexible part of the copolymer. For a rubberlike material $g(T)$ would simply read

$$g(T) \propto kT \tag{2A}$$

$h(T)$ contains the effect of temperature on the number of "effective links" per unit volume. Assuming that partial melting takes place at T_M, we choose to write $h(T)$ as follows:

$$h(T) \propto C_{prep}/C_\alpha \quad \text{for} \quad T < T_M \tag{3A}$$

$$h(T) \propto [C_{prep} - C_{MI}(T)]/[C_{\alpha s}(T) - C_{MI}(T)] \quad \text{for} \quad T > T_M \tag{4A}$$

where $C_{\alpha s}(T)$ is the concentration defined by the solidus at T ($C_{\alpha s} = C_\alpha$ at $T = T_M$) and $C_{MI}(T)$ that defined by the liquidus ($C_{MI}(T) = C_M$ at $T = T_M$). This is equivalent to saying that $h(T)$ and correspondingly the number of "effective links" are directly proportional to the amount of polymer-rich phase.

By approximating $g(T) \simeq Cte$ and $f(C) \simeq Cte$ within the range of temperatures investigated, $E(T)/E(20)$ reads

$$E(T)/E(20) = 1 \quad \text{for} \quad T < T_M \tag{5A}$$

$$E(T)/E(20) = [(C_{prep} - C_{MI}(T))/(C_{\alpha s}(T) - C_{MI}(T))] \times (C_\alpha/C_{prep}) \quad \text{for} \quad T > T_M \tag{6A}$$

To simplify the numerical calculations of $C_{\alpha s}(T)$ and $C_{MI}(T)$, a schematic phase diagram is used (Figure 14). In this diagram, the liquidus line is approximated to a straight line and two different solidus lines are considered. Otherwise, C_M and C_α are taken from the experimental data and T_M is taken 5 °C lower than its value measured at 20 °C/min to correct for the heating rate effect.[28] In Figure 15 is drawn the numerical simulations and the experimental points. The agreement is particularly good by taking the solidus line 2.

Obviously, this theory is mainly phenomenological at the moment and will accordingly require from now on deeper molecular insight. Although unsophisticated, this approach clearly points out what was suspected on the melting mechanism.

Appendix B

The equilibrium swelling ratio reads

$$G^\infty = (P/P_0)_{t\to\infty} \tag{1B}$$

The sample's weight P can be expressed as:

$$P = P_0 + \Pi \tag{2B}$$

where Π is the amount of solvent incorporated on swelling. Assuming that this amount of solvent is directly proportional to the amount of polymer-rich phase X_α, then Π reads

$$\Pi = (C_\alpha/C_\gamma - 1)X_\alpha P_0 \tag{3B}$$

where C_γ is the concentration reached by the polymer-rich phase after swelling or equilibrium.

Eventually, G^∞ reads

$$G^\infty = 1 + (C_\alpha/C_\gamma - 1)X_\alpha \tag{4B}$$

X_α simply reads for $T < T_M$:

$$X_\alpha = (C_{prep} - C_l)/(C_{\alpha s} - C_l) \tag{5B}$$

where C_l and $C_{\alpha s}$ are the concentrations defined by the liquidus and the solidus lines, respectively. By approximation of $C_{\alpha s} = C_\alpha$ and $C_l = 0$, X_α becomes

$$X_\alpha = C_{prep}/C_\alpha \tag{6B}$$

References and Notes

(1) Lemstra, P. J.; Challa, G. *J. Polym. Sci., Polym. Phys. Ed.* **1975**, *13*, 1809. Girolamo, M.; Keller, A.; Miyasaka, K.; Overbergh, N. *J. Polym. Sci., Polym. Phys. Ed.* **1976**, *14*, 39. Wellinghoff, S. J.; Shaw, J.; Baer, E. *Macromolecules* **1979**, *12*, 932. Sundararajan, P. R.; Tyrer, N. J.; Bluhm, T. L. *Macromolecules* **1982**, *15*, 286. Guenet, J. M.; Lotz, B.; Wittmann, J. C. *Macromolecules* **1985**, *18*, 420.

(2) Tan, H. M.; Hiltner, A.; Moet, H.; Baer, E. *Macromolecules* **1983**, *16*, 28. Gan, Y. S.; François, J.; Guenet, J. M. *Macromolecules* **1986**, *19*, 173.

(3) Guerrero, S. J.; Keller, A. *J. Macromol. Sci., Phys.* **1981**, *B20*, 167. Harrison, M. A.; Morgan, P. H.; Park, G. S. *Eur. Polym. J.* **1972**, *8*, 1361. Dorrestijn, A.; Keijzers, A. E.; te Nijenhuis, K. *Polymer* **1981**, *22*, 305. Yang, Y. C.; Geil, P. H. *J. Macromol. Sci., Phys.* **1983**, *B22*, 463.

(4) Delmas, G.; et al. *Macromolecules* **1984**, *17*, 1200; **1985**, *18*, 1235.

(5) Smith, P.; Lemstra, P. J. *J. Mater. Sci.* **1980**, *15*, 505.

(6) Stamhuis, J. E.; Pennings, A. J. *Br. Polym. J.* **1978**, *10*, 221. Toyama, K.; Miller, W. G. *Nature (London)* **1981**, *289*, 813.

(7) Berghmans, H.; Govaerts, F.; Overbergh, N. *J. Polym. Sci., Polym. Phys. Ed.* **1979**, *17*, 1251.

(8) Takahashi, A. *Polym. J.* **1973**, *4*, 379. Domszy, R. C.; Alamo, R.; Edwards, C. O.; Mandelkern, L. *Macromolecules* **1986**, *19*, 310.

(9) Prud'homme, C. Thesis, Strasbourg, **1980**.

(10) Bargain, M.; Prud'homme, C. Ger. Offen., 1979, 2 901 514; *Chem. Abstr.* **1979**, *91*, 141946d.

(11) Chaumont, P.; Beinert, G.; Herz, J.; Rempp, P. *Eur. Polym. J.* **1979**, *15*, 459.

(12) Macosco, C. W.; Benjamin, G. S. *Pure Appl. Chem.* **1981**, *53*, 1505.

(13) Fisher, A.; Gottlieb, M. 8th Polymer Networks Group Meeting; Elsinore, Denmark, 1986.

(14) He, X. W.; Lapp, A.; Herz, J., unpublished results.

(15) He, X. W.; Fillon, B.; Herz, J.; Guenet, J. M. *Polym. Bull. (Berlin)* **1987**, *17*, 45.

(16) Belkebir-Mrani, A.; Herz, J.; Rempp, P. *Makromol. Chem.* **1977**, *178*, 485.

(17) Carbonnel, L.; Rosso, J. C.; Ponge, C. *Bull. Soc. Chim. (Fr.)* **1972**, *3*, 941.

(18) Cahn, J. W. *J. Am. Ceram. Soc.* **1969**, *52*, 118.

(19) Schaaf, P.; Lotz, B.; Wittmann, J. C. *Polymer* **1987**, *28*, 193.

(20) Guenet, J. M. *Macromolecules* **1986**, *19*, 1961.

(21) He, X. W.; Herz, J.; Guenet, J. M., unpublished results.

(22) Janacek, J.; Ferry, J. D. *Macromolecules* **1969**, *2*, 379.

(23) Guenet, J. M.; McKenna, G. B. *J. Polym. Sci., Polym. Phys. Ed.* **1986**, *24*, 2499.

(24) de Gennes, P.-G. In *Scaling Concepts in Polymer Physics*; Cornell University: Ithaca, NY, 1979.

(25) See, for instance: Bastide, J. Thesis, Strasbourg, 1985.

(26) Munch, J. P.; Candau, S. J.; Hild, G.; Herz, J. *J. Phys. (Paris)* **1977**, *58*, 971.

(27) Beltzung, M.; Herz, J.; Picot, C. *Macromolcules* **1983**, *16*, 580.

(28) Guenet, J. M.; Picot, C. *Macromolecules* **1983**, *16*, 2.